

Published in final edited form as:

Ann Surg. 2010 October ; 252(4): 625–634. doi:10.1097/SLA.0b013e3181f5a079.

## Identification of E-Selectin as a Novel Target for the Regulation of Post-Natal Neovascularization: Implications for Diabetic Wound Healing

Zhao-Jun Liu, PhD<sup>1,2</sup>, Runxia Tian, MD<sup>1</sup>, Weijun An, MD<sup>1</sup>, Ying Zhuge, MD<sup>1</sup>, Yan Li, BS<sup>1</sup>, Hongwei Shao, MD<sup>1</sup>, Bianca Habib, BS<sup>1</sup>, Alan S. Livingstone, MD<sup>1</sup>, and Omaida C. Velazquez, MD<sup>1,2,\*</sup>

<sup>1</sup>Department of Surgery, Miller School of Medicine, University of Miami, Miami, FL, 33136

<sup>2</sup>Sylvester Comprehensive Cancer Center, University of Miami, Miami, FL, 33136

### Abstract

**Objectives**—We previously reported that stromal cell-derived factor-1 $\alpha$  (SDF-1 $\alpha$ , a homing signal for recruiting endothelial progenitor cells (EPC) to areas of neovascularization), is down-regulated in diabetic wounds <sup>1</sup>. We now investigate signals whereby mature endothelial cells (EC) and circulating EPC achieve SDF-1 $\alpha$ -mediated EPC homing.

**Methods**—SDF-1 $\alpha$  in diabetic wounds were therapeutically increased by injection of SDF-1 $\alpha$ -engineered bone marrow-derived fibroblasts versus control cells (N= 48 (20, NOD), (28, STZ-C57)). PCR-array gene expression differences were validated by Western blotting and immunohistochemistry. The role of adhesion molecule(s) in mediating SDF-1 $\alpha$ -induced EPC homing and wound healing was furthered studied using antagonists *in vitro* and *in vivo*.

**Results**—Increasing wound SDF-1 $\alpha$  via cell-base therapy promotes healing in diabetic mice (~20% increase in healing rates by day 3,  $p=0.006$ ). SDF-1 $\alpha$  increased EC-EPC adhesion and specifically upregulated E-selectin expression in human microvascular EC (2.3-fold increase,  $p<0.01$ ). This effect was also significant in blood vessels of the experimental mice and resulted in increased wound neovascularization. The regulatory effects of SDF-1 $\alpha$  on EC-EPC adhesion and EPC homing were specifically mediated by E-selectin, as the application of E-selectin antagonists significantly inhibited SDF-1 $\alpha$ -induced EC-EPC adhesion, EPC homing, wound neovascularization, and wound healing.

**Conclusions**—SDF-1 $\alpha$ -engineered cell-based therapy promotes diabetic wound healing in mice by specifically upregulating E-selectin expression in mature EC leading to increase EC-EPC adhesion, EPC homing and increased wound neovascularization. These findings provide novel

\*Correspondence and request for reprint: Omaida C. Velazquez, MD, FACS, Chief, Division of Vascular & Endovascular Surgery, Associate Professor of Surgery, The DeWitt Daughtry Family Department of Surgery, Leonard M. Miller school of Medicine, The University of Miami, 1611 NW 12th Avenue, East Tower 3016, Miami, FL 33101-6310, Phone: 305-585-5284 Fax: 305-585-8569, ovelazquez@med.miami.edu.

**Publisher's Disclaimer:** This is a PDF file of an unedited manuscript that has been accepted for publication. As a service to our customers we are providing this early version of the manuscript. The manuscript will undergo copyediting, typesetting, and review of the resulting proof before it is published in its final citable form. Please note that during the production process errors may be discovered which could affect the content, and all legal disclaimers that apply to the journal pertain.

Type of study: This work is preclinical research on the effects of E-Selectin and SDF-1 $\alpha$  on neovascularization and wound healing in diabetic murine models and on mechanisms of action for these effects.

Disclosure: Data from this and other prior work in this area of investigation has led to the filing of two Patent applications: "E-Selectin Alone or in Combination with SDF-1 For Enhancing Wound Healing" Inventors: OC Velazquez and Zhao-Jun Liu; provisional Patent application filed April 21, 2009 (61/171,271); and "SDF-1A and HBO2 for treatment of diabetic ulcerations" Inventors: OC Velazquez and Katherine Gallagher; provisional Patent application filed March 22, 2007 (P-9680-USP (201621)

insight into the signals underlying the biological effect of SDF-1 $\alpha$  on EPC homing and point to E-selectin as a new potential target for therapeutic manipulation of EPC trafficking in diabetic wound healing.

---

## Introduction

Restoring blood flow to the site of injured tissue is a prerequisite for mounting a successful repair response. It is now well established that the sources of endothelial cells which build newly-formed blood vessels come from both pre-existing vessels (angiogenesis) and bone marrow-derived EPC (vasculogenesis). In addition to direct cellular contribution to new vessels, EPC secrete growth factors and cytokines that enhance angiogenesis and other wound healing processes via paracrine effects. EPC are the key cellular effectors of both reparative and pathologic postnatal neovascularization and play a pivotal role in not only wound healing, but also limb ischemia<sup>2-4</sup>, post-myocardial infarction<sup>5-7</sup>, endothelialization of vascular grafts<sup>8,9</sup>, atherosclerosis<sup>10</sup>, retinal and lymphoid organ neovascularization<sup>11,12</sup>, vascularization during neonatal growth<sup>13</sup>, and tumor growth<sup>14,15</sup>.

The recruitment of EPC from the bone marrow and circulation to sites of neovascularization by the process known as “homing” is subject to regulation by many factors, including chemokines and growth factors. SDF-1 $\alpha$  is the predominant chemokine that acts as a potent homing signal for EPC<sup>16</sup>. We have previously demonstrated that the local concentration of SDF-1 $\alpha$  in diabetic wounds is significantly decreased. Epithelial cells and myofibroblasts appear to be responsible for the down-regulation of SDF-1 $\alpha$  in diabetic wounds, while the exogenous administration of SDF-1 $\alpha$  to wounds of diabetic mice increase the wound-level EPC recruitment and directly impact wound angiogenesis/vasculogenesis, collagen deposition, and wound closure rates<sup>1</sup>. SDF-1 $\alpha$  is a chemoattractant that exerts its role through binding with its receptor C-X-C chemokine receptor 4 (CXCR4), which is expressed on the cell surface of EPC<sup>17</sup> and may function as a sensor for circulating EPC cruising through sites of the microvasculature wherein an SDF-1 $\alpha$  gradient is present. In fact, inhibition of the SDF-1 $\alpha$ /CXCR4 interaction partially blocks the homing of progenitor/stem cells to the ischemic myocardium<sup>18</sup>. Thus, it has been well accepted that the SDF-1 $\alpha$ /CXCR4 axis plays a critical role in guiding the trafficking of EPC, though the exact mechanism(s) remained unknown, until the work presented herein. We reasoned that since SDF-1 $\alpha$  itself is a soluble factor, even if it binds to CXCR4 on the surface of the circulating EPC, it would be unable to directly mediate attachment of EPC to the EC monolayer lining the blood vessel lumen within the microvasculature of a wound. Thus, under the shear force of the blood flow, circulating EPC would be unlikely to adhere to the EC monolayer. In this study we hypothesized that direct cell-cell interactions are required between the EC lining the capillaries and the circulating EPC in order to achieve EPC homing to the target tissues, and that the effect of SDF-1 $\alpha$  on EPC homing is mediated, at least partially, by regulating specific adhesion molecule(s) on EC monolayers. We aimed to identify such an adhesion molecule(s) which could mediate SDF-1 $\alpha$ -induced homing of EPC. We demonstrated that SDF-1 $\alpha$  specifically upregulates the expression of E-selectin in murine and human mature EC monolayers. E-selectin is responsible for mediating the effect of SDF-1 $\alpha$  on EPC homing by enhancing adhesion of EPC to EC monolayers and their transendothelial migration. Importantly, these effects result in significant enhancement of wound neovascularization and wound healing.

## Materials and Methods

### Cells

Human microvascular endothelial cells (HMVEC), kindly provided by Dr. D. Fraker, University of Pennsylvania, Philadelphia, PA, were isolated from normal human dermis and

cultured as described<sup>19</sup> on plates coated with 1% gelatin. Human EPC were purchased from NDRI, Philadelphia, PA, and cultured in complete EGM2 medium containing supplements and 5% fetal bovine serum (FBS) (Cambrex Bioscience, Walkersville, MD). 293, 293T and NIH/3T3 cells were cultured in DMEM (Invitrogen, Carlsbad, CA) supplemented with 10% FBS. All cells were incubated at 37°C in 98% humidified air containing 5% CO<sub>2</sub>. For cell adhesion and transendothelial migration assays, EPC were labeled with Dil-Ac-LDL (BT-902, Biomedical Technologies, Stoughton, MA) for 4 hours at 37°C, and washed with phosphate-buffered saline (PBS). Subconfluent HMVEC or EPC were stimulated with recombinant human SDF-1 $\alpha$  (100 ng/ml) for various times as indicated in the experiments. BSA (100 ng/ml) was used as control.

## Mice

All procedures were done with approval from the University of Miami Institutional Animal Care and Use Committee. Wild-type (WT) female C57 BL6 mice at 8–12 weeks of age were purchased from Charles River (Wilmington, MA). 10–12-week old NOD (NOD/shilTJ), 8-week old E-sel<sup>-/-</sup> (B6.129S4-sele<sup>tm1Dmil/J</sup>) mice and 10–12-week old Rosa26 (lacZ<sup>+</sup>) (B6.129S7-GT (ROSA)26sor/J) mice were purchased from the Jackson Laboratory (Bar Harbor, ME). For all surgical procedures, mice were anesthetized with an i.p. injection of 80 mg/kg of ketamine and 20 mg/kg xylazine. For bone marrow transplantation experiments,  $1 \times 10^7$  bone marrow cells from Rosa26 mice were suspended in 100  $\mu$ l of PBS and transplanted into E-sel<sup>-/-</sup> or WT mice (C57 BL6) through tail vein injection.

## Induction of diabetes plus generation of peripheral cutaneous wounds

Streptozocin (STZ, Sigma-Aldrich) diabetes was induced and monitored as previously described<sup>1</sup>. NOD mice usually developed diabetes within 14–20 weeks. A total of 48 diabetic mice (N=28, STZ-C57; N=20, NOD) were studied. Serum glucose was measured from the mouse tail vein using a glucometer. Once serum glucose reached 250 mg/dl, mice were followed with daily measurements for 3 days prior to use in experiments. Mean serum glucose levels in diabetic mice were 446 mg/dl with a range of 356–512 mg/dl, while mean serum glucose levels in control non-diabetic mice were 122 mg/dl with a range of 96–137 mg/dl. Wounds were induced on the dorsal surface of the mouse back using a 6-mm punch biopsy. Full-thickness skin was removed, exposing the underlying muscle.

## Recombinant lentiviruses and adeno-associated viruses (AAV)

Based on prior studies documenting optimal viral transduction efficiency and on projected potential clinical relevance<sup>20</sup>, we selected lentivirus vectors for *in vitro* studies and adeno-associated virus vectors for *in vivo* experiments, as tools for manipulating levels of SDF-1 $\alpha$ . Human SDF-1 $\alpha$ /lenti was constructed by inserting the human or murine *SDF-1 $\alpha$*  genes into pHX vector<sup>21</sup>. Control vector, GFP/lenti was constructed as described previously<sup>22</sup>. Production of pseudotyped lentivirus was achieved by co-transfecting 293 T cells with three plasmids as described<sup>23</sup>. The lentiviruses collected 48 hours post-transfection displayed titers of around  $10^7$  transducing units/ml in NIH/3T3 cells. To infect target cells by lentiviruses, cells were exposed for six hours to virus with MOI (multiplicity of infection) 5 in the presence of 4  $\mu$ g/ml polybrene (Sigma-Aldrich). Cells were then washed, cultured with regular complete medium for two additional days, and analyzed for protein expression by ELISA or pooled for subsequent analysis as indicated in individual experiments. Murine SDF-1 $\alpha$ /AAV and control vector, LacZ/AAV were constructed by inserting the murine *SDF-1 $\alpha$*  or *LacZ* gene into AAV2 vector<sup>24</sup>. Production of AAV was achieved by transfecting 293 cells with three plasmids and AAV was purified by heparin chromatography method and titrated as previously described<sup>25</sup>. For local wound injections with recombinant AAV, 100  $\mu$ l of AAV at  $10^{12}$  viral unit/ml in PBS was injected into the wound base. For cell-based therapy, bone marrow-derived fibroblasts (BMDFs) were

created by culturing murine bone marrow cells on plastic dish in DMEM medium supplemented with 10% FBS for two weeks with medium changes every 3 days. Adherent cells displayed spindle shape and are  $\alpha$ -smooth muscle actin<sup>+</sup> ( $\alpha$ SMC<sup>+</sup>) (data not shown) consistent with the myofibroblast phenotype. BMDFs were transduced with lentiviral vectors encoding murine SDF-1 $\alpha$  or GFP (as control). Expression of exogenous mSDF-1 $\alpha$  in BMDFs was confirmed by ELISA (Supplemental Digital Figure 1). 6-mm punch biopsy skin wounds were created and  $1 \times 10^7$  mSDF-1 $\alpha$ /BMDFs versus GFP/BMDFs suspended in 100  $\mu$ l of PBS were injected into the wound.

### PCR array

The Human Adhesion Molecules & ECM *RT<sup>2</sup> Profiler<sup>TM</sup> PCR Array* quantitatively profiles the expression of 84 genes of adhesion molecules and ECM (# PA-011, SABiosciences, Frederick, MD). Subconfluent HMVEC were stimulated with recombinant human SDF-1 $\alpha$  protein versus BSA at 100ng/ml for 4 hours. Cells were harvested and total RNA was extracted from cells using Trizol<sup>®</sup> (Invitrogen) and cDNA was synthesized using RT<sup>2</sup> First Strand Kits (SABiosciences). PCR array was carried out according to the manufacturer's protocol. The threshold cycle (Ct) values were used to plot a standard curve. All samples were normalized to the relative levels of  $\beta$ -actin, and results are expressed as fluorescence intensity in relative levels.

### ELISA

Concentration of SDF-1 $\alpha$  in the supernatant of cell culture was measured by Quantikine<sup>®</sup> SDF-1 $\alpha$  ELISA kit (DY460, R&D Systems), which specifically detects murine SDF-1 $\alpha$ , based on the manufacturer's protocol.

### Cell adhesion assay

EC-monolayers of HMVEC were cultured in 24-well plate to near confluency and stimulated with recombinant human SDF-1 $\alpha$  or BSA at 100 ng/ml for 8 hours. Subsequently, culture medium was replaced with SDF-1 $\alpha$ -free EGM2 medium.  $1 \times 10^5$  Dil-Ac-LDL-labeled EPC, which were pre-labeled and cultured on 2% agarose-coated plate as suspension for 16 hours, were added into wells and co-cultured with the HMVEC monolayer for 1 hour at 37 °C. Unbound EPC were washed out by PBS twice and adherent Dil-Ac-LDL-labeled EPC were measured by fluorescence scanner (GE Typhoon Trio, Piscataway, NJ) and photographed.

### Cell transendothelial migration assay

$1 \times 10^4$  cells/well of HMVEC were cultured in the upper chamber of a fibronectin (5  $\mu$ g/ml)-coated 24- transwell insert (8.0- $\mu$ m pores; Falcon 353097, Becton Dickinson Bedford, MA). Before each experiment, monolayer confluency was confirmed by inverted fluorescence microscopy. The HMVEC monolayers were stimulated with recombinant human SDF-1 $\alpha$  or BSA at 100 ng/ml for 8 hours.  $1 \times 10^4$  Dil-Ac-LDL-labeled EPC, which were pre-labeled as detailed above, were added into the upper chamber in 0.3 mL basal EGM2 medium. 0.6 mL complete EGM2 medium was added to the lower chamber of the transwell. Cells were cultured for 12 hours at 37°C, and EPC traversing from the upper to the lower chamber of the transwell were quantified.

### Immunoblotting, immunostaining and immunohistochemistry

Immunoblotting was performed as described<sup>26</sup>. Membranes were probed with antibodies (Abs) to E-selectin (ab-18981) or  $\beta$ -actin (AC-15, Abcam, Cambridge, MA). This was followed by probing with HRP-conjugated secondary Ab (Santa Cruz, Santa Cruz, CA) and

subjected to ECL (Amersham Biosciences, Piscataway, NJ). Membranes were stripped and re-blotted as required in the individual experiments.

For immunostaining and immunohistochemistry (IHC), 5- $\mu$ m paraffin or frozen sections were processed as described<sup>21</sup> and were then incubated with FITC-anti-E-selectin (R&D Systems), PE-anti-KDR (Cell Signaling Technology, Danvers, MA) or anti-SDF-1 $\alpha$  (sc28876, Santa Cruz) for overnight at 4°C, then incubated with HRP-conjugated secondary antibodies. Immunoreactivity was detected using DAB kit (Dako, Carpinteria, CA). The nuclei were counterstained with either DAPI (Vector Labs, Burlingame, CA) or hematoxylin (IHC). Negative controls for all antibodies were made by replacing the primary antibodies with non-immunogen, isotype matched Abs from the same manufacturer.

### **Induction of hindlimb ischemia plus generation of peripheral cutaneous wounds**

To induce limb ischemia, the full length (about 3–4 mm) of the right femoral artery/vein vascular bundle were ligated and excised (two groups of mice were studied: E-selectin<sup>-/-</sup> mice (n=6) and WT mice (n=6)). The skin was then closed with 5-0 nylon (Ethicon). Limb ischemia was confirmed by Laser Doppler perfusion imaging. Ischemic hindlimb wounds were induced on the ventral surface of the thigh of the mouse using a 4mm punch biopsy. A full thickness section of skin was removed, exposing the underlying muscle distal to the level of the femoral fold. Recombinant murine SDF-1 $\alpha$  protein (R&D Systems) was reconstituted in PBS and injected into the wound base (25 $\mu$ g/kg) right after the surgery.

### **Assessment of Wound Closure Rate**

Wounds were followed serially with daily digital photographs using an Olympus digital camera. A ruler was included in all photos to allow for calibration of measurements. Images were analyzed using ImageJ software (Imaging Processing and Analysis in Java, National Institutes of Health, MD). Wound area was measured each day, and the wound's percent recovery rate was expressed as [(original wound area minus daily wound area)/(original wound area)] X 100.

### **Blood Vessel Perfusion and Laser Scanning Confocal Microscopy**

Mouse blood vessels were directly labeled *in vivo* in anesthetized mice by live perfusion using a specially formulated aqueous solution (7 ml/mouse) containing DiI (D-282, Invitrogen/Molecular Probes), which incorporates into endothelial cell membranes upon contact, and was administered via direct intra-cardiac injection prior to animal sacrifice as previously reported<sup>27</sup>. Seven ml of fixative (4% paraformaldehyde) was injected following DiI perfusion and the entire wound tissue was harvested. The vascular network was visualized by scanning the entire wound tissue to a thickness or depth of 200  $\mu$ m, using laser scanning confocal microscopy (Vibratome (VT1000S, Leica Microsystems). Vessel density was quantified assessing total number of red DiI-labelled vessels normalized to the entire scanned wound area, using ImageJ software.

### **Laser Doppler Perfusion Imaging (LDI)**

Limb perfusion was assessed daily using LDI (Periscan PIM II, Perimed AB, Sweden). The limb was defined as all imaged tissue distal to the femoral fold of the mouse. LDI was performed in a temperature controlled facility with weight based sedation to minimize artifacts due to temperature fluctuations and level of sedation. Relative perfusion data were expressed as the ratio of the ischemic (right) to normal (left) limb blood flow.

## Bone Marrow Transplantation and $\beta$ -Galactosidase Assay for Tissue-Level Detection of bone marrow-derived EPC

$1 \times 10^7$  bone marrow cells from 10~12-week old Rosa26 (LacZ<sup>+</sup>) mice were engrafted into E-sel<sup>-/-</sup> mice (n=6) and WT mice (n=6) through tail vein injection right after creation of ischemic hindlimb wounds (right limb). The number of LacZ<sup>+</sup> EPC recruited to wound tissues and integrated into blood vessels in tissue sections were quantified by  $\beta$ -galactosidase assay. Harvested wound tissues were frozen and tissue sections were then incubated with X-gal (Fermentas, Canada) and anti-KDR (ab-2349, Abcam) for 2 hours at room temperature. Sections were counterstained with nuclear fast red (Vector Labs). The number of EPC was quantified by counting  $\beta$ -galactosidase<sup>+</sup> cells in KDR<sup>+</sup> vessels in serial sections of wound granulation tissues underlying the excisional wounds at post-operative day 7 (n=3) in 5 random high power fields (HPF, 40X) per section in at least 3 serial sections.

### Statistical Analyses

Statistical analysis of differences was performed using ANOVA and 2-tail Student's *t*-test. Data was analyzed using Microsoft Excel (Microsoft Corp, Redmond, WA). Data is expressed as mean  $\pm$  standard error. Values are considered statistically significant when  $p < 0.05$ .

## Results

### 1. SDF-1 $\alpha$ -engineered cell-based therapy promotes cutaneous wound neovascularization and diabetic wound healing

We previously reported that tissue levels of SDF-1 $\alpha$  in diabetic murine wounds were significantly decreased, partly due to its down-regulation in myofibroblasts<sup>1</sup>. In this study, we sought to test efficacy of SDF-1 $\alpha$ -engineered cell-based therapy for diabetic wound healing. The purpose is to test the pro-healing effect of fibroblast-derived SDF-1 $\alpha$  on diabetic wound healing in a genetic (NOD) diabetes murine model. BMDFs were selected, as mature resident cutaneous fibroblasts in patients with diabetes associated wounds are known to be impaired and thus carry little clinical relevance as potential therapeutic vehicle. Diabetic wounds treated with mSDF-1 $\alpha$ /BMDFs were completely healed significantly faster than those injected with GFP/BMDFs (Figure 1A). Similar pro-healing results were observed in STZ-C57 diabetic mice with cutaneous wounds (data not shown). The naked vector treatment of wounds also showed a pro-healing response but not as pronounced as with the cell-based approach (Supplemental Digital Figure 2). The most significant difference was observed at day 4 and 5. Correspondingly, significantly more active neovascularization developed in wounds treated with mSDF-1 $\alpha$ /BMDFs compared to the control wounds as demonstrated by confocal laser scanning microscopy of wounds after blood vessel perfusion with Dil dye (Figure 1B). Wounds were harvested and subjected to IHC analysis. Stronger expression of SDF-1 $\alpha$  in wounds injected with mSDF-1 $\alpha$ /BMDFs versus GFP/BMDFs was confirmed by IHC (Figure 1C). These results confirmed a pro-healing and pro-angiogenic effects of SDF-1 $\alpha$  in diabetic murine models and provided preclinical evidence that SDF-1 $\alpha$ -engineered cell-based therapy may serve as a novel tool for the treatment of diabetic wounds.

### 2. Enhanced adhesion of human EPC to SDF-1 $\alpha$ -stimulated EC monolayer in vitro

To test our hypothesis that the effect of SDF-1 $\alpha$  on EPC homing is mediated by regulating adhesion molecule(s) on mature endothelial cells, we first examined whether SDF-1 $\alpha$  stimulation could make an EC monolayer more likely to support adhesion of EPC in an *in vitro* cell-cell adhesion assay. Subconfluent HMVEC were stimulated with recombinant

human SDF-1 $\alpha$  or BSA. Dil-Ac-LDL-labeled EPC were added into wells and co-cultured with EC-monolayer. Unbound EPC were washed out and adherent Dil-Ac-LDL-labeled EPC were measured by fluorescence scanner (Figure 2A). There was approximately an 8-fold increase in the number of EPC adherent to the SDF-1 $\alpha$ -stimulated EC monolayers compared to BSA-treated control (Figure 2B). This data indicated that SDF-1 $\alpha$  stimulation promotes direct EPC-EC adhesion, suggesting that the expression of certain adhesion molecule(s) on EC may be specifically regulated by SDF-1 $\alpha$ .

### 3. SDF-1 $\alpha$ stimulation up-regulates expression of E-selectin in EC monolayers (in vitro) and wound capillary endothelium of mice (in vivo)

To identify the adhesion molecule(s) up-regulated by SDF-1 $\alpha$  in EC monolayers, we carried out RT<sup>2</sup> Profiler™ PCR array. Of the 84 genes tested in the array, 13 were up-regulated (> 1.5-fold) while 20 down-regulated (<1.5-fold) and 51 were unaltered (Table 1). Notably, the expression of *E-selectin* gene was increased about 2.3-fold upon SDF-1 $\alpha$  stimulation (Figure 3A). To validate the observed up-regulation of mRNA of *E-selectin*, we conducted immunoblotting analyses and confirmed an up-regulated protein expression of E-selectin in SDF-1 $\alpha$ -stimulated compared to BSA-treated EC monolayers (Figure 3B). To further validate the up-regulation of E-selectin by SDF-1 $\alpha$  in mature endothelial cells *in vivo*, we examined vessels in diabetic NOD mice wounds injected with mSDF-1 $\alpha$ /AAV versus lacZ/AAV by immunostaining. EC of blood vessels in diabetic murine wounds injected with mSDF-1 $\alpha$ /AAV expressed stronger E-selectin compared to those injected with LacZ/AAV (Figure 3C). Increased tissue levels in mSDF-1 $\alpha$ /AAV was demonstrated by IHC (Figure 3D). These experiments identified E-selectin as one key adhesion molecule that is up-regulated as a down-stream target of SDF-1 $\alpha$  in vascular EC.

### 4. Up-regulated E-selectin is responsible for mediating SDF-1 $\alpha$ -enhanced EC-EPC interaction and EPC transendothelial migration

To study whether up-regulated E-selectin is responsible for mediating SDF-1 $\alpha$ -enhanced EC-EPC adhesion, we tested the effect of E-selectin antagonist on EPC adhesion to SDF-1 $\alpha$ -stimulated EC monolayer *in vitro*. Subconfluent HMVEC stimulated with recombinant human SDF-1 $\alpha$  or BSA was cultured with SDF-1 $\alpha$ -free EGM2 medium containing either E-selectin neutralizing Ab or isotype-matched control Ab (2  $\mu$ g/ml) and incubated for 15 minutes at 37 °C before adding EPC. Subsequently, Dil-Ac-LDL-labeled EPC were added into the wells and co-cultured with the EC-monolayer. Unbound EPC were washed out and adherent Dil-Ac-LDL-labeled EPC were measured by fluorescence scanner. The addition of E-selectin neutralizing Ab significantly inhibited the number of EPC adherent to SDF-1 $\alpha$ -stimulated EC monolayers whereas control Ab had no significant effect (Figure 4A). To further investigate the biological function of E-selectin in mediating a specific interaction between EPC and the EC monolayer, we tested whether increased adhesion between EPC and the EC monolayer results in more EPC transmigrating through the EC monolayers, and if yes, whether this transmigration effect is E-selectin-dependent. EPC transendothelial migration was tested in an *in vitro* transwell system. HMVEC monolayers were cultured in the upper chamber of transwell inserts in the presence of  $\gamma$ hSDF-1 $\alpha$  or BSA. Fifteen minutes prior to adding EPC into the insert, EGM2 medium in the lower chamber was replaced with fresh medium containing  $\gamma$ hSDF-1 $\alpha$  or BSA, respectively. Dil-Ac-LDL-labeled EPC suspension were added into the insert and cultured for overnight. Compared to BSA-treated EC monolayers, SDF-1 $\alpha$ -stimulated EC monolayers showed significantly increased EPC transmigration from the upper to the lower transwell chamber (Figure 4B). Importantly, this effect is, at least partially, E-selectin-dependent, since blockade of E-selectin by adding neutralizing Ab (2  $\mu$ g/ml) to the transwell was able to significantly inhibit EPC transendothelial migration (Figure 4B). Overall, these

results demonstrated that up-regulated E-selectin is responsible for mediating SDF-1 $\alpha$ -enhanced EC-EPC adhesion and EPC transendothelial migration.

### 5. SDF-1 $\alpha$ stimulation up-regulates expression of E-selectin ligands in EPC

Ultimately, the direct interaction between EC lining the wound's capillaries and the circulating EPC would depend upon mutually relevant counterparts of adhesion molecules on the surface of both cell types. We hypothesized that SDF-1 $\alpha$  might induce expression of relevant adhesion molecule(s) on both EC and EPC. Based on the results detailed above that SDF-1 $\alpha$ -induced E-selectin on EC mediates direct EC-EPC interactions, we specifically examined the expression of two E-selectin ligands, CD44 and CD162 (PSGP-1), on EPC in response to SDF-1 $\alpha$  stimulation. Subconfluent human EPC were stimulated with  $\gamma$ hSDF-1 $\alpha$  or BSA, respectively, for various periods of time. Cells were harvested and subjected to immunoblotting analyses. Unstimulated EPC expressed strong basal levels of CD162 and low levels of CD44. SDF-1 $\alpha$  stimulation up-regulated expression of both CD162 and CD44 in EPC (Figure 5). Induction of CD162 and CD44 was first observed in 4 hours upon SDF-1 $\alpha$  stimulation and continued to increase until 16 hours. These experiments confirmed that EPC express basal levels of E-selectin ligands and show that SDF-1 $\alpha$  is able to up-regulate the expression of these E-selectin ligands in EPC, consistent with the overall hypothesis that the soluble factor, SDF-1 $\alpha$ , mediates EPC homing effects by specifically regulating the profile of adhesion molecules on these two key cell types, the mature endothelial cell and the EPC.

### 6. E-selectin is required for mediating effects of SDF-1 $\alpha$ on EPC homing, neovascularization and wound healing in murine ischemic hindlimb and cutaneous wound model

To study the specific biological importance of SDF-1 $\alpha$ -induced E-selectin in EPC homing, neovascularization, and cutaneous wound healing, we employed a loss-of-function approach in combination with bone marrow transplantation. A murine model of unilateral hindlimb ischemia via femoral ligation/excision and subsequent bilateral 4-mm cutaneous excisional wounding was created in E-selectin<sup>-/-</sup> versus WT mice. Recombinant murine SDF-1 $\alpha$  was administered to wounds via direct wound injections. Further treatment was provided by engrafting bone marrow cells from Rosa26(LacZ<sup>+</sup>) mice into mice via the tail vein, to quantify (partially) the contribution of EPC homing to neovascularization and wound healing. LDI was used to confirm post-operative limb ischemia, and monitor and quantify the spontaneous restoration of hindlimb blood flow via mean perfusion measured over time. Daily wound area measurements were obtained via digital photography. Neovascularization in wound tissues was evaluated by blood vessel DiI perfusion and subsequent laser scanning confocal microscopy in harvested wound tissues in half of experimental mice at day 7. In the remaining mice, the wounds were harvested and subjected to IHC. EPC recruited to wound tissues and incorporated into blood vessels were detected by double staining with  $\beta$ -gal (blue) and anti-KDR. Compared to WT mice, ischemic hindlimbs in E-selectin<sup>-/-</sup> mice showed delayed improvements in perfusion over time as indicated by the significantly lower mean flux measurements (Figure 6A). Consistently, ischemic wounds in E-selectin<sup>-/-</sup> mice had significantly slower closure rate that in WT mice (Figure 6B). In addition, ischemic wounds in E-selectin<sup>-/-</sup> mice were much more poorly vascularized compared to those in WT mice (Figure 6C). The poor neovascularization in ischemic wounds of E-selectin<sup>-/-</sup> mice was, at least partially, related to fewer EPC homing, since significantly less LacZ<sup>+</sup> cells were detected in blood vessels of ischemic wounds in the E-selectin<sup>-/-</sup> mice compared to the WT mice (Figure 6D). These *in vivo* experiments demonstrated that E-selectin is required for mediating SDF-1 $\alpha$ -induced EPC homing, neovascularization and wound healing.



## Discussion

In the present study we have demonstrated that SDF-1 $\alpha$  carries significant relevance as a potential new target to enhance diabetic wound healing and that the effect of SDF-1 $\alpha$  on enhancing EPC homing, neovascularization, and wound healing is mediated by the upregulation of E-selectin expression on endothelial cells as well as the upregulation of corresponding E-selectin ligands on the EPC. Thus, E-selectin may be a potential new target in the unsolved epic problem of diabetes-associated cutaneous impaired wound healing. These data demonstrate that SDF-1 $\alpha$  increases expression of E-selectin on the luminal surface of mature endothelial cells and thereby creates a microenvironment that promotes adhesion and transendothelial migration of EPC. These effects, in turn, promote limb and wound neovascularization and enhance wound healing.

The microvasculature in the granulation tissue of cutaneous wounds is physically supported by connective tissue elements elaborated by resident fibroblasts. These fibroblasts provide a unique microenvironment that facilitates and sustains the newly formed vessels. Fibroblasts and their activated counterpart, the myofibroblasts, play a pivotal role in regulating neovascularization in the process of wound healing by synthesis of extracellular matrix (ECM) and secreting various soluble factors<sup>28–31</sup>. Myofibroblasts can either arise from the local, resident fibroblasts or from circulating mesenchymal precursors/stem cells<sup>32,33</sup>. Recently, cell-based therapy has become a promising novel option to improve vascularization or tissue regeneration<sup>34</sup>. Using cell-based therapy we have shown that engrafting SDF-1 $\alpha$ -engineered bone marrow-derived fibroblasts into diabetic wounds, where tissue levels of SDF-1 $\alpha$  are known to be down-regulated<sup>1</sup>, can significantly improve tissue levels of E-selectin on endothelial cells and promote wound neovascularization and wound healing in different murine diabetic wound models (STZ and NOD). Cell-based therapy showed improved healing effects, in our murine models, compared to gene therapy, suggesting that bone marrow-derived fibroblasts can provide additional beneficial effects on wound healing. We had previously reported the contribution of EPC to enhanced neovascularization in an STZ-induced murine diabetic wound model<sup>1</sup>. This most current work demonstrates that this effect of SDF-1 $\alpha$  is also seen in NOD mice and is E-selectin-dependent, as less EPC recruitment along with poor neovascularization and poor wound healing occurred in the ischemic wounds of E-selectin<sup>-/-</sup> mice compared to that in WT mice despite local wound administration of recombinant SDF-1 $\alpha$  protein. Our overall prior and current results implicate E-selectin as a target that could be modulated to enhance EPC-associated neovascularization and healing in diabetes associated wounds.

E-selectin is only minimally expressed constitutively in the unstimulated/quiescent EC. Thus, the basal level of E-selectin expressed on the luminal surface of blood vessels is likely insufficient for circulating EPC to be captured in the “homing” process. Some pro-inflammatory cytokines, such as TNF- $\alpha$  and IL-1, can induce vascular expression of E-selectin<sup>35</sup>. For example, E-selectin is known to be involved in the interaction of leukocytes and the endothelial cell lining of blood vessels for leukocyte transendothelial migration in inflammation. Our findings that E-selectin is required for EPC-EC interaction in post-natal EPC-mediated neovascularization support the novel hypothesis that EPC may utilize adhesion molecules for their homing to sites of damaged tissues similar to the adhesion molecules engaged by leukocyte recruitment to sites of inflammation<sup>36,37</sup>. It appears rational that sharing common adhesion molecules for both EPC and leukocyte homing is resource efficient for the body, and in fact, in many cases, inflammatory cells are recruited along with reparative progenitor cells to sites of damaged tissues wherein neovascularization as well as inflammatory cell-mediated mechanisms against contamination and infection are needed, although no obvious inflammation was noted in our experimental wounds.

E-selectin is only one of several adhesion molecules that are up-regulated by SDF-1 $\alpha$  stimulation in vascular EC monolayers. In addition to E-selectin, several other adhesion molecules, such as VCAM-1 and integrin  $\alpha$ 4, were also induced. It is likely that more than one of these adhesion molecules are involved in orchestrating the dynamic process of EPC homing which involves EPC rolling, firm adhesion to the EC monolayer and subsequent transendothelial migration. Additionally, since EPC homing is a complex and dynamic process involving cell–cell and cell-ECM engagement and disengagement a spatiotemporal manner, it is not surprising that some adhesion molecules need to be down-regulated. In fact, we observed that 20 genes were down-regulated by SDF-1 $\alpha$  stimulation. In this study, we focused on E-selectin because it has also been previously reported to be involved in EPC homing to ischemic muscle<sup>38</sup>. Our study not only confirms the critical role of E-selectin in EPC homing from a novel perspective never previously realized (diabetes-associated cutaneous wounds), but also reveals for the first time that upregulated E-selectin mediates SDF-1 $\alpha$ -induced EPC homing. Given our prior findings on the connection between the diabetic phenotype and the cutaneous wound down-regulation of SDF-1 $\alpha$ , these novel data point to E-selectin as a new target in the field of diabetes impaired wound healing. The functional relevance of other listed adhesion molecules/ECM requires further study.

There are three known ligands capable of interacting with E-selectin, and we examined two of them (CD162 and CD44). Similar to mature endothelial cells expressing low basal levels of E-selectin, the EPC express low basal levels of CD162 and CD44 as well. The significance of the detected low basal level expression of these adhesion molecules is unclear. Nevertheless, these low levels are likely insufficient to bring about significant EPC-EC interaction under unstimulated conditions. Interestingly, the two examined E-selectin ligands on EPC are responsive to SDF-1 $\alpha$  stimulation. Thus, it is possible that SDF-1 $\alpha$  produced in wounded tissue in response to hypoxia inducible factor (HIF-1  $\alpha$ ) upregulation in the wound's relative hypoxic microenvironment<sup>39</sup> can stimulate both local EC and circulating EPC to express adhesion molecules and thereby enhance EPC-EC interactions that result in EPC homing. Our new proposed working model is that the circulating EPC get stimulated when they pass through the “swampy” low-flow vessels of the injured tissue wherein a specific profile of adhesion molecules are upregulated under the influence of SDF-1 $\alpha$  that promotes the homing process. When these stimulated EPC come back to the site on re-circulation, they are “captured” or become adherent to the “sticky” EC surface of the wound's capillary beginning the processes of transendothelial migration and EPC extravasation that are required for EPC homing. In this sequence of events, E-selectin may play a central role.

## Conclusion

Our experiments demonstrated that SDF-1 $\alpha$  specifically upregulates the expression of E-selectin in mature EC and E-selectin ligands on EPC, thereby mediating EC-EPC adhesion and EPC homing. These findings provide profound and novel insight into the molecular mechanism underlying the biological effect of SDF-1 $\alpha$  on EPC homing and point to E-selectin as a new potential target for therapeutic manipulation of EPC homing in diabetes-associated microangiopathy and delayed wound healing. The modulation of E-selectin and its ligands in EC and EPC may offer an opportunity to not only regulate the EPC-associated direct angiogenic response, but also, the associated direct and indirect effects on wound healing that are intrinsically relevant to the unsolved clinical problem of delayed diabetes-associated cutaneous wound healing. Our findings could be developed into a new translational platform for subsequent clinical trials. Successful completion of clinical testing may offer a novel paradigm for advancing and transforming the field of diabetic wound care, and eliminate the need for over 100, 000 major limb amputations per year at a health care cost that exceeds 2 Billion dollars, yearly, in the US alone.

## Supplementary Material

Refer to Web version on PubMed Central for supplementary material.

## Acknowledgments

Sources of support: This work was supported by grants from the National Institutes of Health (R01DK-071084 and R01GM081570), and a grant from the Wallace H. Coulter Center for Translational Research, University of Miami. The equipment used in this study belongs to the Department of Surgery, and core facilities of the University of Miami Miller School of Medicine. No pharmaceutical drugs were used in this work.

We thank Dr. D. Fraker for kindly providing HMVEC and Dr. George McNamara for assistance with laser scanning confocal microscopy and image quantification.

## References

- Gallagher KA, Liu ZJ, Xiao M, Chen H, Goldstein LJ, Buerk DG, Nedeau A, Thom SR, Velazquez OC. Diabetic impairments in NO-mediated endothelial progenitor cell mobilization and homing are reversed by hyperoxia and SDF-1 alpha. *J Clin Invest.* 2007; 117:1249–1259. [PubMed: 17476357]
- Majka SM, Jackson KA, Kienstra KA, Majesky MW, Goodell MA, Hirschi KK. Distinct progenitor populations in skeletal muscle are bone marrow derived and exhibit different cell fates during vascular regeneration. *J Clin Invest.* 2003; 111:71–79. [PubMed: 12511590]
- Kalka C, Masuda H, Takahashi T, Kalka-Moll WM, Silver M, Kearney M, Li T, Isner JM, Asahara T. Transplantation of ex vivo expanded endothelial progenitor cells for therapeutic neovascularization. *Proc Natl Acad Sci U S A.* 2000; 97:3422–3427. [PubMed: 10725398]
- Takahashi T, Kalka C, Masuda H, Chen D, Silver M, Kearney M, Magner M, Isner JM, Asahara T. Ischemia- and cytokine-induced mobilization of bone marrow-derived endothelial progenitor cells for neovascularization. *Nat Med.* 1999; 5:434–438. [PubMed: 10202935]
- Orlic D, Kajstura J, Chimenti S, Bodine DM, Leri A, Anversa P. Transplanted adult bone marrow cells repair myocardial infarcts in mice. *Ann N Y Acad Sci.* 2001; 938:221–229. discussion 229–230. [PubMed: 11458511]
- Orlic D, Kajstura J, Chimenti S, Jakoniuk I, Anderson SM, Li B, Pickel J, McKay R, Nadal-Ginard B, Bodine DM, Leri A, Anversa P. Bone marrow cells regenerate infarcted myocardium. *Nature.* 2001; 410:701–705. [PubMed: 11287958]
- Kocher AA, Schuster MD, Szabolcs MJ, Takuma S, Burkhoff D, Wang J, Homma S, Edwards NM, Itescu S. Neovascularization of ischemic myocardium by human bone-marrow-derived angioblasts prevents cardiomyocyte apoptosis, reduces remodeling and improves cardiac function. *Nat Med.* 2001; 7:430–436. [PubMed: 11283669]
- Shi Q, Rafii S, Wu MH, Wijelath ES, Yu C, Ishida A, Fujita Y, Kothari S, Mohle R, Sauvage LR, Moore MA, Storb RF, Hammond WP. Evidence for circulating bone marrow-derived endothelial cells. *Blood.* 1998; 92:362–367. [PubMed: 9657732]
- Kaushal S, Amiel GE, Guleserian KJ, Shapira OM, Perry T, Sutherland FW, Rabkin E, Moran AM, Schoen FJ, Atala A, Soker S, Bischoff J, Mayer JE Jr. Functional small-diameter neovessels created using endothelial progenitor cells expanded ex vivo. *Nat Med.* 2001; 7:1035–1040. [PubMed: 11533707]
- Sata M, Saiura A, Kunisato A, Tojo A, Okada S, Tokuhisa T, Hirai H, Makuuchi M, Hirata Y, Nagai R. Hematopoietic stem cells differentiate into vascular cells that participate in the pathogenesis of atherosclerosis. *Nat Med.* 2002; 8:403–409. [PubMed: 11927948]
- Otani A, Kinder K, Ewalt K, Otero FJ, Schimmel P, Friedlander M. Bone marrow-derived stem cells target retinal astrocytes and can promote or inhibit retinal angiogenesis. *Nat Med.* 2002; 8:1004–1010. [PubMed: 12145646]
- Grant MB, May WS, Caballero S, Brown GA, Guthrie SM, Mames RN, Byrne BJ, Vaught T, Spoerri PE, Peck AB, Scott EW. Adult hematopoietic stem cells provide functional hemangioblast activity during retinal neovascularization. *Nat Med.* 2002; 8:607–612. [PubMed: 12042812]

13. Young PP, Hofling AA, Sands MS. VEGF increases engraftment of bone marrow-derived endothelial progenitor cells (EPCs) into vasculature of newborn murine recipients. *Proc Natl Acad Sci U S A*. 2002; 99:11951–11956. [PubMed: 12195016]
14. Lyden D, Hattori K, Dias S, Costa C, Blaikie P, Butros L, Chadburn A, Heissig B, Marks W, Witte L, Wu Y, Hicklin D, Zhu Z, Hackett NR, Crystal RG, Moore MA, Hajar KA, Manova K, Benezra R, Rafii S. Impaired recruitment of bone-marrow-derived endothelial and hematopoietic precursor cells blocks tumor angiogenesis and growth. *Nat Med*. 2001; 7:1194–1201. [PubMed: 11689883]
15. Reyes M, Dudek A, Jahagirdar B, Koodie L, Marker PH, Verfaillie CM. Origin of endothelial progenitors in human postnatal bone marrow. *J Clin Invest*. 2002; 109:337–346. [PubMed: 11827993]
16. Lapidot T. Mechanism of human stem cell migration and repopulation of NOD/SCID and B2mnull NOD/SCID mice. The role of SDF-/CXCR4 interactions. *Ann N Y Acad Sci*. 2001; 938:83–95. [PubMed: 11458529]
17. Walter DH, Haendeler J, Reinhold J, Rochwalsky U, Seeger F, Honold J, Hoffmann J, Urbich C, Lehmann R, Arenzana-Seisdesdos F, Aicher A, Heeschen C, Fichtlscherer S, Zeiher AM, Dimmeler S. Impaired CXCR4 signaling contributes to the reduced neovascularization capacity of endothelial progenitor cells from patients with coronary artery disease. *Circ Res*. 2005; 97:1142–1151. [PubMed: 16254213]
18. Abbott JD, Huang Y, Liu D, Hickey R, Krause DS, Giordano FJ. Stromal cell-derived factor-alpha plays a critical role in stem cell recruitment to the heart after myocardial infarction but is not sufficient to induce homing in the absence of injury. *Circulation*. 2004; 110:3300–3305. [PubMed: 15533866]
19. Liu ZJ, Snyder R, Soma A, Shirakawa T, Ziober BL, Fairman RM, Herlyn M, Velazquez OC. VEGF-A and alphaVbeta3 integrin synergistically rescue angiogenesis via N-Ras and PI3-K signaling in human microvascular endothelial cells. *Faseb J*. 2003; 17:1931–1933. [PubMed: 14519669]
20. Lundstrom K. Gene therapy applications of viral vectors. *Technol Cancer Res Treat*. 2004; 3:467–477. [PubMed: 15453812]
21. Balint K, Xiao M, Pinnix CC, Soma A, Veres I, Juhasz I, Brown EJ, Capobianco AJ, Herlyn M, Liu ZJ. Activation of Notch1 signaling is required for beta-catenin-mediated human primary melanoma progression. *J Clin Invest*. 2005; 115:3166–3176. [PubMed: 16239965]
22. Liu ZJ, Xiao M, Balint K, Smalley KS, Brafford P, Qiu R, Pinnix CC, Li X, Herlyn M. Notch1 signaling promotes primary melanoma progression by activating mitogen-activated protein kinase/phosphatidylinositol 3-kinase-Akt pathways and up-regulating N-cadherin expression. *Cancer Res*. 2006; 66:4182–4190. [PubMed: 16618740]
23. Liu ZJ, Xiao M, Balint K, Soma A, Pinnix CC, Capobianco AJ, Velazquez OC, Herlyn M. Inhibition of endothelial cell proliferation by Notch1 signaling is mediated by repressing MAPK and PI3K/Akt pathways and requires MAML1. *FASEB J*. 2006; 20:1009–1011. [PubMed: 16571776]
24. Gao G, Vandenberghe LH, Wilson JM. New recombinant serotypes of AAV vectors. *Curr Gene Ther*. 2005; 5:285–297. [PubMed: 15975006]
25. Gao G, Qu G, Burnham MS, Huang J, Chirmule N, Joshi B, Yu QC, Marsh JA, Conceicao CM, Wilson JM. Purification of recombinant adeno-associated virus vectors by column chromatography and its performance in vivo. *Hum Gene Ther*. 2000; 11:2079–2091. [PubMed: 11044910]
26. Liu ZJ, Shirakawa T, Li Y, Soma A, Oka M, Dotto GP, Fairman RM, Velazquez OC, Herlyn M. Regulation of Notch1 and Dll4 by vascular endothelial growth factor in arterial endothelial cells: implications for modulating arteriogenesis and angiogenesis. *Mol Cell Biol*. 2003; 23:14–25. [PubMed: 12482957]
27. Li Y, Song Y, Zhao L, Gaidosh G, Laties AM, Wen R. Direct labeling and visualization of blood vessels with lipophilic carbocyanine dye DiI. *Nat Protoc*. 2008; 3:1703–1708. [PubMed: 18846097]
28. Tomasek JJ, Gabbiani G, Hinz B, Chaponnier C, Brown RA. Myofibroblasts and mechano-regulation of connective tissue remodelling. *Nat Rev Mol Cell Biol*. 2002; 3:349–363. [PubMed: 11988769]

29. Velazquez OC, Snyder R, Liu ZJ, Fairman RM, Herlyn M. Fibroblast-dependent differentiation of human microvascular endothelial cells into capillary-like 3-dimensional networks. *FASEB J*. 2002; 16:1316–1318. [PubMed: 12060671]
30. Kalluri R, Zeisberg M. Fibroblasts in cancer. *Nat Rev Cancer*. 2006; 6:392–401. [PubMed: 16572188]
31. Hinz B, Phan SH, Thannickal VJ, Galli A, Bochaton-Piallat ML, Gabbiani G. The myofibroblast: one function, multiple origins. *Am J Pathol*. 2007; 170:1807–1816. [PubMed: 17525249]
32. De Wever O, Mareel M. Role of tissue stroma in cancer cell invasion. *J Pathol*. 2003; 200:429–447. [PubMed: 12845611]
33. Direkze NC, Hodivala-Dilke K, Jeffery R, Hunt T, Poulson R, Oukrif D, Alison MR, Wright NA. Bone marrow contribution to tumor-associated myofibroblasts and fibroblasts. *Cancer Res*. 2004; 64:8492–8495. [PubMed: 15574751]
34. Perin EC, Geng YJ, Willerson JT. Adult stem cell therapy in perspective. *Circulation*. 2003; 107:935–938. [PubMed: 12600902]
35. Wyble CW, Hynes KL, Kuchibhotla J, Marcus BC, Hallahan D, Gewertz BL. TNF-alpha and IL-1 upregulate membrane-bound and soluble E-selectin through a common pathway. *J Surg Res*. 1997; 73:107–112. [PubMed: 9441802]
36. Luster AD, Alon R, von Andrian UH. Immune cell migration in inflammation: present and future therapeutic targets. *Nat Immunol*. 2005; 6:1182–1190. [PubMed: 16369557]
37. Ley K, Laudanna C, Cybulsky MI, Nourshargh S. Getting to the site of inflammation: the leukocyte adhesion cascade updated. *Nat Rev Immunol*. 2007; 7:678–689. [PubMed: 17717539]
38. Oh IY, Yoon CH, Hur J, Kim JH, Kim TY, Lee CS, Park KW, Chae IH, Oh BH, Park YB, Kim HS. Involvement of E-selectin in recruitment of endothelial progenitor cells and angiogenesis in ischemic muscle. *Blood*. 2007; 110:3891–3899. [PubMed: 17699745]
39. Ceradini DJ, Kulkarni AR, Callaghan MJ, Tepper OM, Bastidas N, Kleinman ME, Capla JM, Galiano RD, Levine JP, Gurtner GC. Progenitor cell trafficking is regulated by hypoxic gradients through HIF-1 induction of SDF-1. *Nat Med*. 2004; 10:858–864. [PubMed: 15235597]

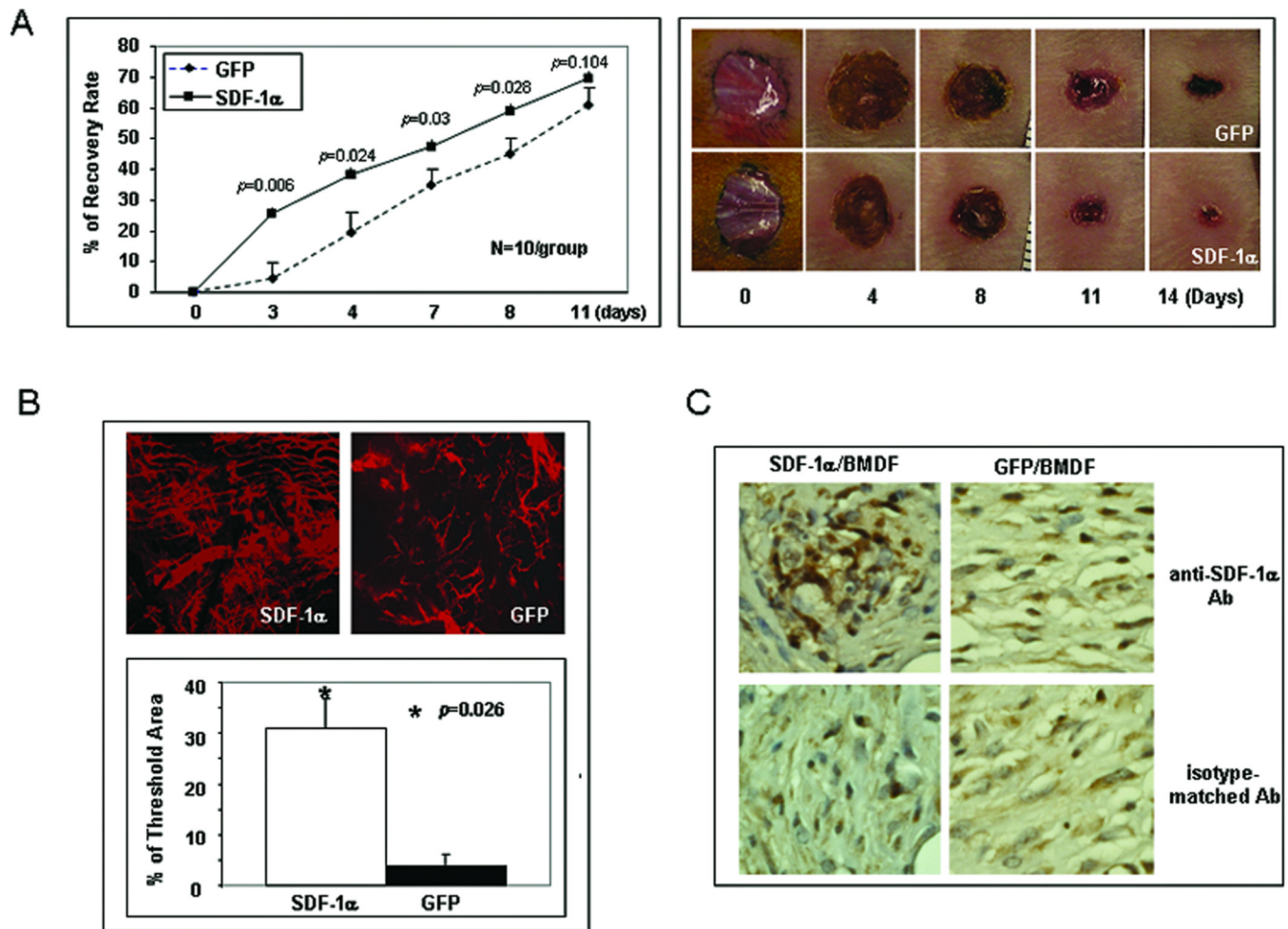
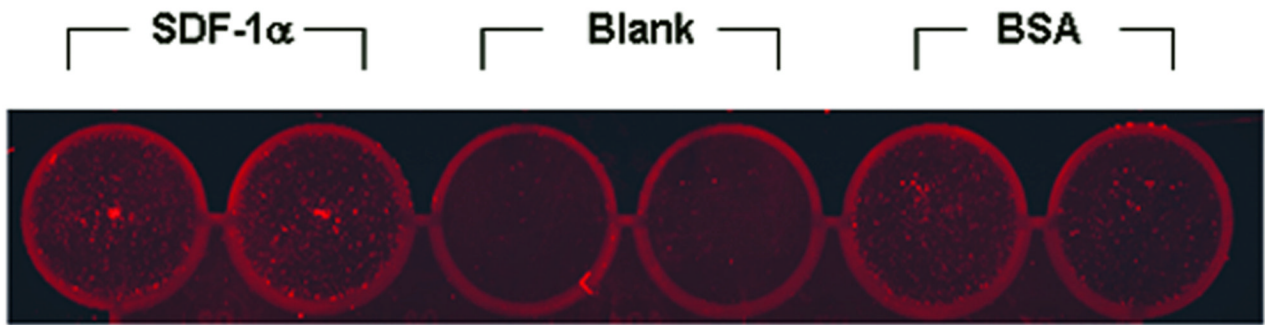


**Figure 1.** SDF-1 $\alpha$ -engineered BMDFs promote neovascularization and diabetic wound healing. (A) *Left:* wound healing rate expressed as percent recovery. Two groups of NOD mice were wounded and treated with mSDF-1 $\alpha$ /BMDFs versus GFP/BMDFs. The fraction of initial wound area was measured daily by digital photography and ImageJ analysis until wounds were healed. Diabetic mice treated with mSDF-1 $\alpha$ /BMDFs had significantly improved wound closure rates from day 3 when compared with GFP/BMDFs treated controls. *Right:* representative wounds at different days are shown for each group. (B) Wound blood vessel perfusion with Dil dye. *Upper:* representative images of Dil-stained wound blood vessels measured by laser scanning confocal microscopy at day 5 are shown for each group. *Lower:* Quantification of vessel density in the wounds. Percentage of threshold area covers all vessels detected as a percent of the entire wound area. mSDF-1 $\alpha$ /BMDFs treated wounds had significantly higher vessel density compared to the control. Data are presented as mean  $\pm$  SD of four wounds in each group. (C) IHC of wound tissues injected with mSDF-1 $\alpha$ /BMDFs versus GFP/BMDFs for the detection of mSDF-1 $\alpha$ . Stronger mSDF-1 $\alpha$  expression (brown) was observed in mSDF-1 $\alpha$ /BMDFs-treated wounds compared to the GFP/BMDFs treated wounds (40X).

A



B

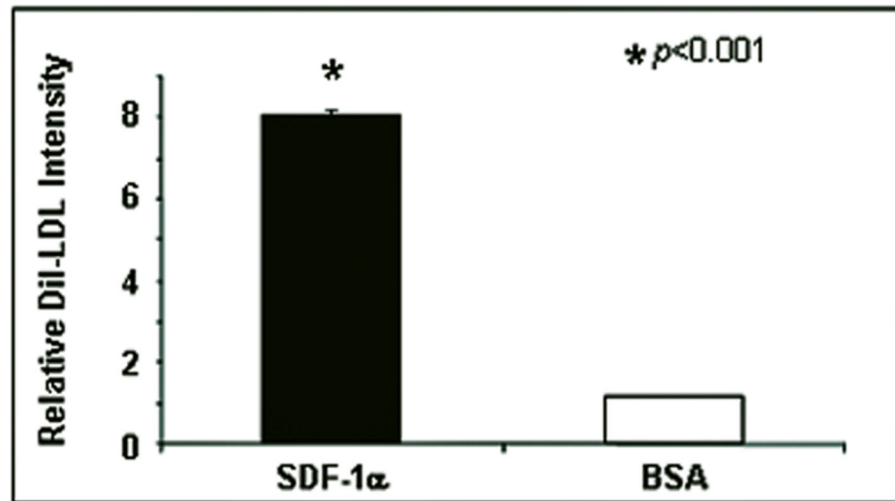


**Figure 2.** Increased adhesion of EPC to SDF-1 $\alpha$ -stimulated EC monolayer *in vitro*. Dil-Ac-LDL-labeled EPC were added to EC monolayers which were stimulated with SDF-1 $\alpha$  or BSA. After 30 min, unbound EPC were washed out. Bound EPC were quantified by fluorescence scanning. (A): representative images. (B): quantitative data. Data are presented as mean  $\pm$  SD of three independent assays in which samples were duplicated.

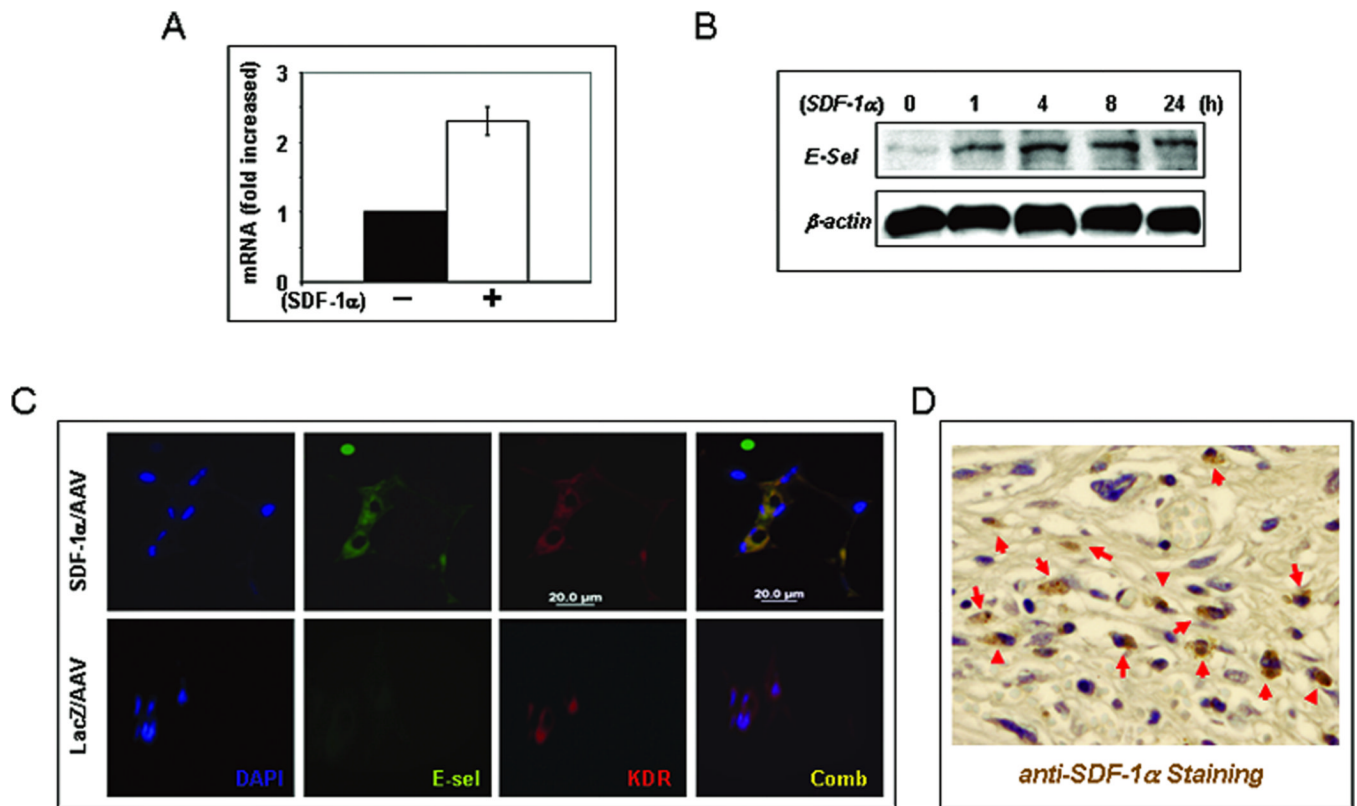


**Figure 3.**

SDF-1 $\alpha$  stimulation up-regulates expression of E-selectin in EC monolayers. (A) HMVEC were stimulated with SDF-1 $\alpha$  or BSA for 4 hours and total RNA were extracted. Expression of extracellular matrix and adhesion molecules were analyzed using *RT2 PCR Array*. Expression of *E-selectin* was upregulated by SDF-1 $\alpha$  stimulation. Levels of mRNA in BSA-treated EC were set as “1” and compared to that in SDF-1 $\alpha$  treated EC. (B): Expression of E-selectin was validated by Western blot analysis. HMVECs were stimulated with SDF-1 $\alpha$  or BSA and cells were harvested at various time points.  $\beta$ -actin was used as loading control. (C) Increased vascular expression of E-selectin in NOD mice wounds injected with mSDF-1 $\alpha$ /AAV compared to that injected with LacZ/AAV. Co-expression (yellow) of KDR (red) and E-selectin (green) in vessels was detected by immunostaining. (D) Increased expression of SDF-1 $\alpha$  in wound tissues-injected with mSDF-1 $\alpha$ /AAV was detected by IHC.



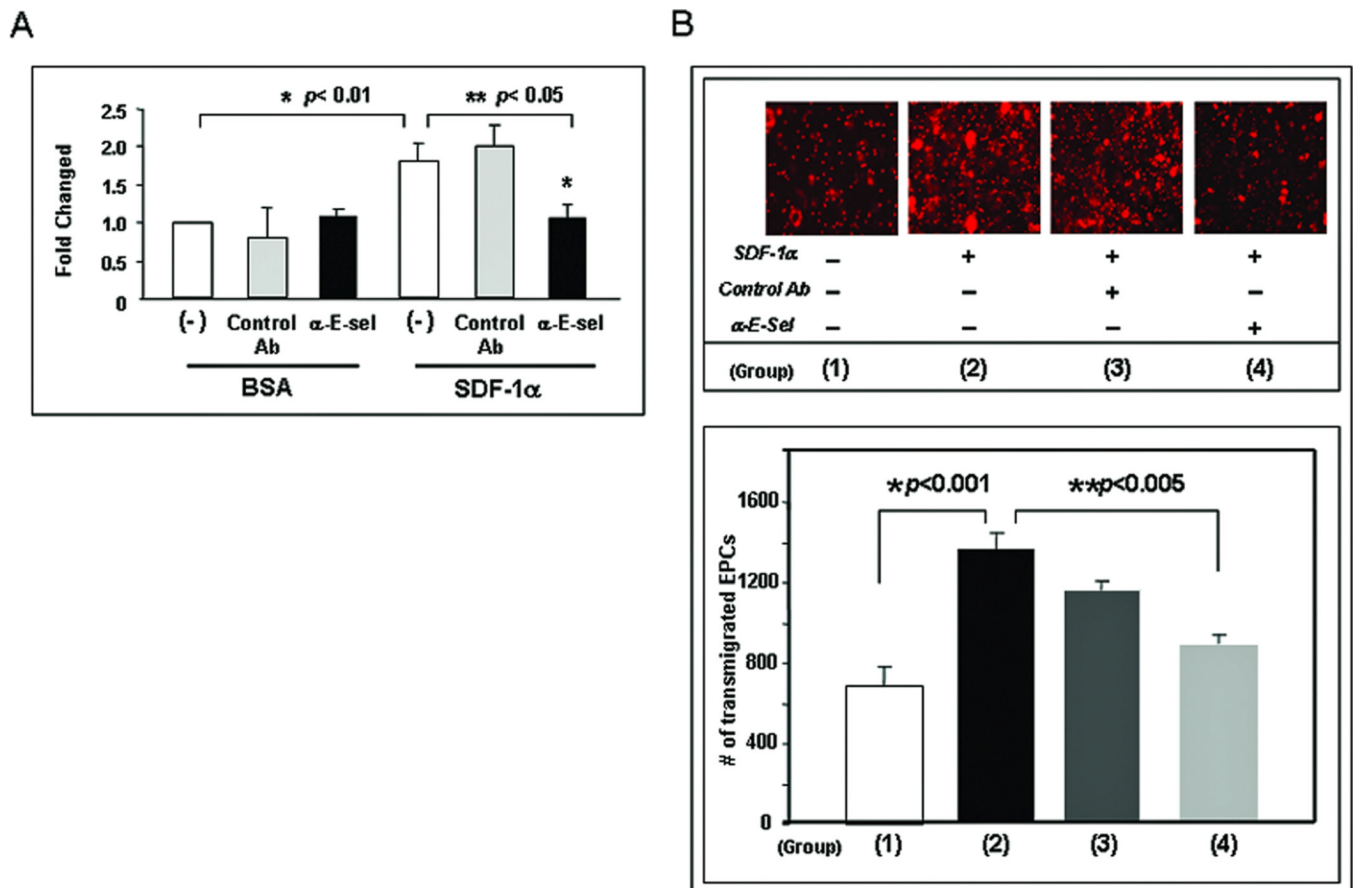


**Figure 4.**

SDF-1 $\alpha$ -induced E-selectin in EC monolayer increases EPC adhesion and transendothelial migration. (A) More EPC adhered to SDF-1 $\alpha$ -stimulated EC monolayer than BSA-treated EC monolayer. Addition of blocking Ab against E-selectin inhibited the interaction of SDF-1 $\alpha$ -stimulated EC with EPC in this cell-cell adhesion assay. Data are presented as mean  $\pm$  SD of three independent assays in which samples were duplicated.

(B, upper panel) Increased numbers of Dil-Ac-LDL labeled EPC were observed to transmigrate to the lower chamber of the transwell with SDF-1 $\alpha$ -stimulated EC monolayer than with BSA-treated EC monolayer. Blocking Ab against E-selectin inhibited this EPC transendothelial migration. (B, lower panel) Dil-EPCs on the lower chamber of the transwell were quantified by fluorescence scanner. Blocking Ab against E-selectin inhibited interaction of SDF-1 $\alpha$ -stimulated EC with EPC. Data are presented as mean  $\pm$  SD of three independent assays in which samples were duplicated.

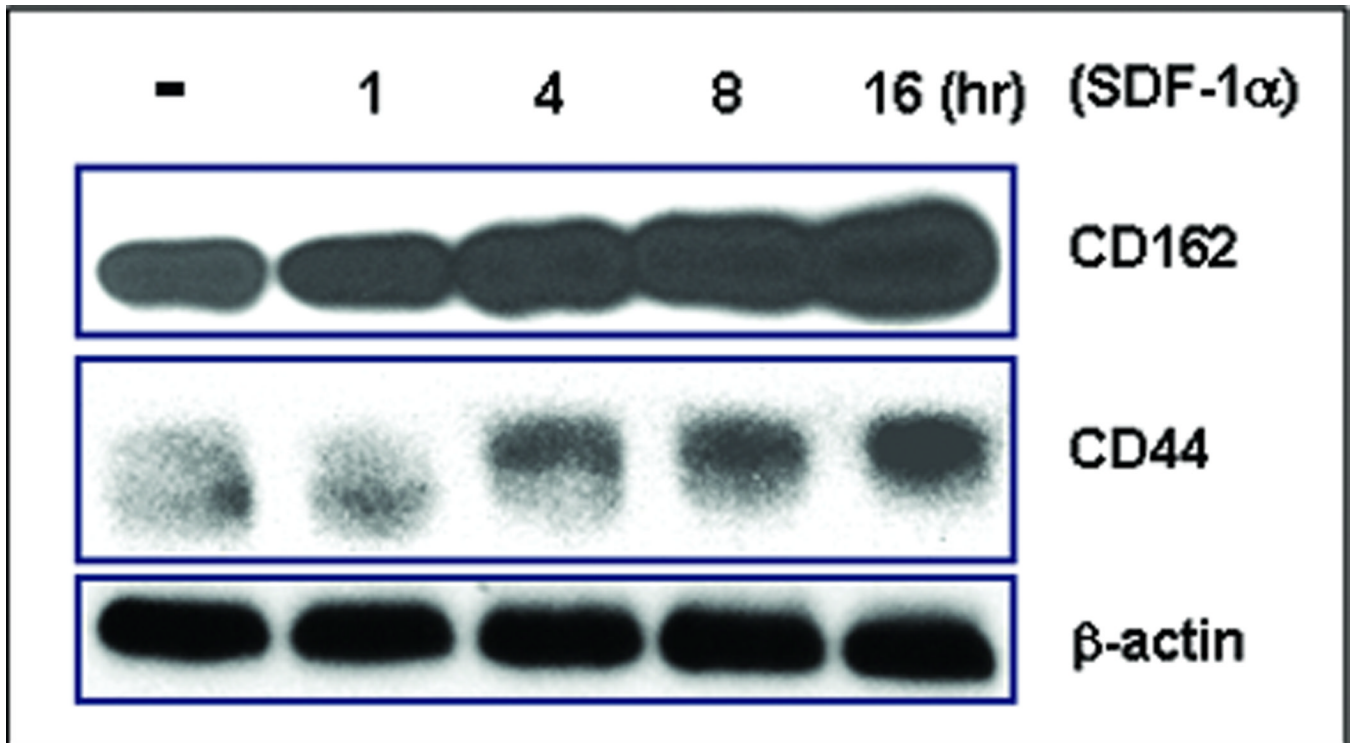


**Figure 5.** SDF-1 $\alpha$  induces expression of E-selectin ligands in EPC. EPC were stimulated by SDF-1 $\alpha$  and cells were harvested at various time points. Expression of E-selectin ligands, CD162 and CD44, was examined by Western blotting assay.  $\beta$ -actin was used as loading control. Experiments were repeated twice.

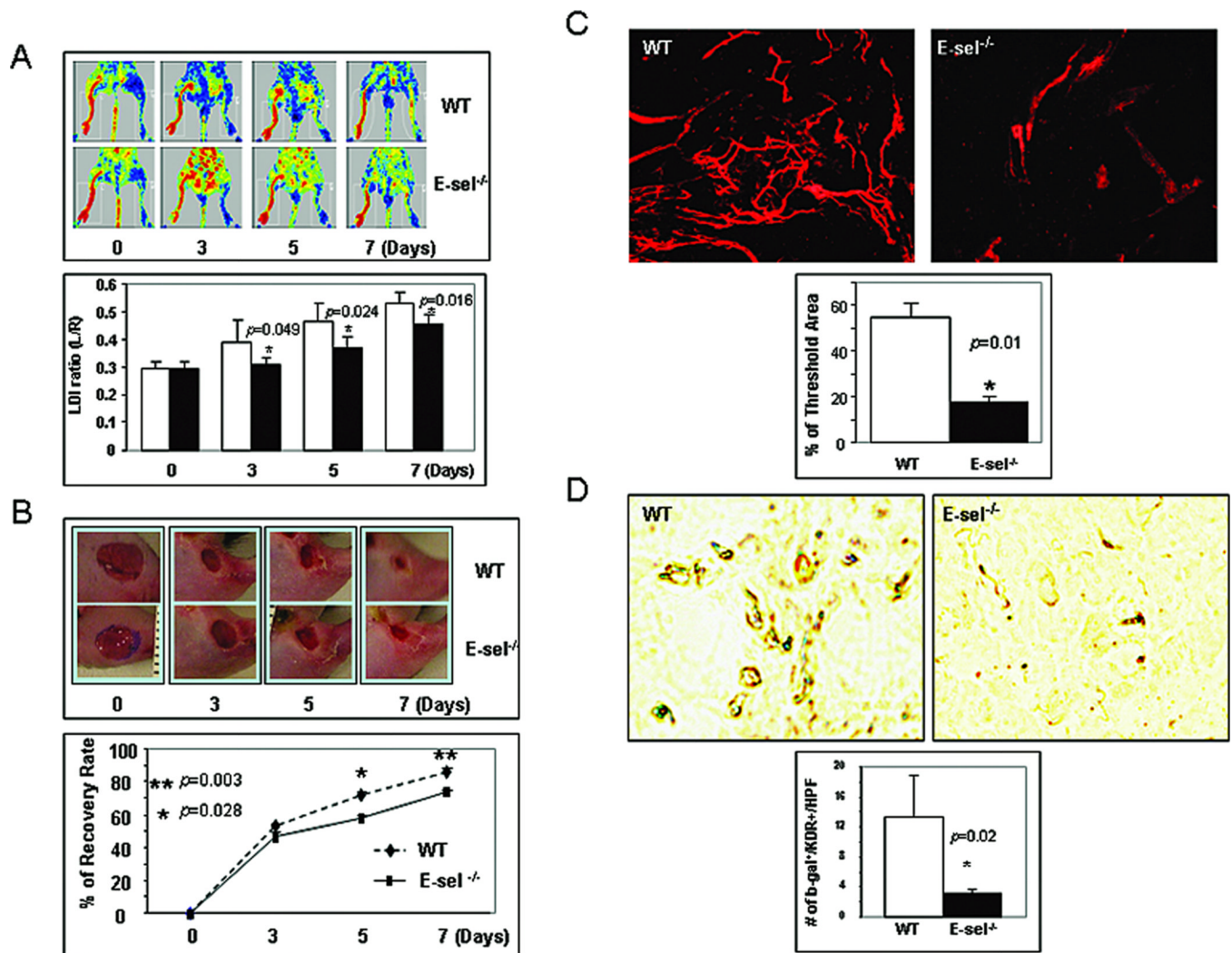


**Figure 6.** Involvement of E-selectin in SDF-1 $\alpha$ -induced EPC homing, neovascularization and wound healing in murine model of hindlimb ischemia plus cutaneous wounding. (A) *Upper*: representative images of non-invasive LDI measurements showing spontaneous restoration of blood flow into ischemic hindlimbs after femoral artery ligation/excision in *E-sel*<sup>-/-</sup> versus WT mice. *Lower*: Quantitative data of LDI measurements. Ratio of ischemic versus normal hindlimb between two groups of mice at various time points. Data are presented as mean  $\pm$  SD from each group (n=6/group). (B) Wound closure rates in *E-sel*<sup>-/-</sup> versus WT. *Upper*: representative images of wound healing in *E-sel*<sup>-/-</sup> and WT mice. Deletion of E-selectin delayed wound healing. *Lower*: Quantitative wound closure rates in *E-sel*<sup>-/-</sup> versus WT mice. Data are presented as percentage wound closure (recovery), mean  $\pm$  SD from each group (n=6/group). (C) Wound blood vessel perfusion with Dil dye. *Upper*: representative images of Dil-stained wound blood vessels detected by confocal laser scanning photography at day 7 are shown for each group. *Lower*: Software-assisted quantification of vessel density in the entire area of residual wounds at day 7, as percent fluorescence. Wounds from WT mice had significantly higher vessel density compared to that from *E-sel*<sup>-/-</sup> mice. Data are presented as mean  $\pm$  SD of three wounds in each group. (D) E-sel is essential for EPC homing to the wound lesion.  $1 \times 10^7$  of bone marrow cells from ROSA26 (LacZ<sup>+</sup>) mice were transplanted to *E-sel*<sup>-/-</sup> and WT mice, respectively. Ischemic hindlimb wounds were

created and SDF-1 $\alpha$  was injected into wounds. 7 days after cell transplantation, wounds were harvested and frozen samples were subjected for X-gal (blue) and anti-KDR (brown) staining. *Upper*: representative images of double staining. *Lower*: number of double positive cells was counted from 5 randomly selected fields in wound samples. Data are percentage of mean  $\pm$  SD from each group (n=3 wounds/group).

**Table 1**Genes up- and down-regulated in 4 hours upon SDF-1 $\alpha$  stimulation in HMVECs.

<b>Up-Regulated</b>	<b>Fold of mRNA changes</b>
CO11A1/COLL6	2.14
CD49D/IA4	1.87
CD49f/ITGA6B	2.14
CD51/DKFZp686A08142	2.3
LAMB2	2
CLG1/HNC	3.73
CD62E/ELAM	2.3
CD62/CD62P	2.3
DYT11/ESG	1.74
BNSP/BSPI	2.14
THBS/TSP	1.74
CLG1/EPA	1.74
CD106/DKFZp779G2333	2.14
<b>Down-Regulated</b>	
CSPG2/DKFZp686K06110	-2.14
CCN2/HCS24	-3.03
CTNNB/DKFZp686D02253	-2.00
CAS/CTNND	-3.73
CIG/DKFZp686F10164	-3.48
BB2/CD54	-2.82
CD49a/VLA1	-4.90
BR/CD49B	-3.03
CD49e/FNRA	-5.30
CD29/FNRB	-2.30
CD61/GP3A	-2.30
FLJ26658	-8.57
LAMM	-2.82
CLM	-2.82
LAMNB1	-5.28
MMP-X2/MT-MMP2	-6.06
CLG4/CLG4A	-4.28
ON	-2.63
CAR/CMAR	-4.00
TSP3	-2.46